JOURNAL OF MATERIALS SCIENCE 22 (1987) 3161–3166

Variations in sintering kinetics and microstructure of alumina with chromium and molybdenum additions

S. V. RAMAN
Brookhaven National Laboratory, Upton, New York 11973, USA

Chromium and molybdenum were introduced into alumina through gel synthesis. Both elements are soluble in aluminium hydroxide and low-temperature (<1400° C) aluminium oxide. In the course of transformation from hydroxide to oxide, the evaporation–condensation of vapour phase (below 1000° C) causes shrinkage of the porous compact due to particle rearrangement and growth through capillary drag and adsorption. Subsequently, differences in agglomerate structure, grain growth, solute atmosphere and densification arise because of variations in the crystallochemical behaviour of chromium and molybdenum. The solute atmospheres of chromia-vacancy and molybdenum metal reveal sub-grain boundaries and dislocations. In chromia–alumina solid solution these defects annihilate and contribute to densification (98%th) with increase in temperature to 1600° C. However, with further rise in temperature to 1700° C, the solid solution desinters to 85%th and creep cavities show transition from grain boundary to lattice creep. In Mo–Al_2O_3 composite the defects are locked by molybdenum solute, and as a result there is an insignificant increase in densification (30%th at 1600° C).

1. Introduction

The addition of solute to alumina is of considerable practical and theoretical importance. For example, increases in fracture strength, electrical resistivity, and magnetic susceptibility have been observed with molybdenum dispersion and chromia solubility [1–3]. On the theoretical side sintering mechanisms have been investigated mostly by MgO addition which seems to have both an inhibiting and enhancing effect on densification, through its influence on variables such as surface energy, mass transport, grain growth and internal pore pressure [4–8]. Another important application involves exploring the influence of defects on sintering by solute-aided lattice ornamentation. For a discussion of such application the reader is referred to Cottrell [9], Gilman and Johnston [10], Cahn [11], Levinstein and Guggenheim [12], and Li and Kingery [13].

In the present study the significance of revealing crystallographic defects by vacancy and chemical atmospheres is realized in view of the plastic flow in alumina [14–18]. Considering the ionic similarity and chemical differences in the reducing atmosphere, chromium and molybdenum seem ideal candidates for creating chromia-vacancy and molybdenum solute atmospheres at higher temperatures [19–21]. The investigation begins with powder synthesis in ethanol solvent for forming homogeneous hydroxide gels of Cr–Al and Mo–Al pairs, respectively. The additive concentrations have been kept low to minimize any extraneous strain that may arise in alumina due to solute segregation. The vapour phase and solute effects on sintering are revealed by X-ray analysis and scanning electron microscopy. The results are compared with those of pure alumina obtained from previous experiments [16, 18]. The results are interpreted to follow the vapour-phase induced particle rearrangement, and the influence of solute on agglomerate structure, phase transformation and creep behaviour.

2. Experimental details

Solutions of 1.8% strength were formed by dissolving in ethanol, the molecular proportions of 12.6% $Cr(NO_3)_3 9H_2O$–87.4% $Al(NO_3)_3 9H_2O$, and 0.16% $(NH_4)_6Mo_7O_{24} 4H_2O$–99.84% $Al(NO_3)_3 9H_2O$. The Cr–Al and Mo–Al hydroxide gels were precipitated from these solutions by stirred addition of NH_4OH (pH = 14) until the titration end point was reached. Following an ageing period of 24 h the supernatant liquid was decanted and the gels were repeatedly cleansed in ethanol. The filtered gelantinous mass was dried to fluffy hydroxide powder in about 100 h at 60° C. The powder was compacted in the double action steel die at a low compacting pressure of approximately 100 p.s.i. (0.689 N mm^{-2}). The cylindrical pellets (0.5 cm height and 1.3 cm diameter) were sintered in the molybdenum-wound furnace in the presence of a flowing hydrogen atmosphere. The temperature was raised from ambient to 1700° C at a constant rate of 5° C min^{-1}. The linear shrinkage and density was determined geometrically. The chemical composition of the sintered pellets was analysed quantitatively by X-ray powder diffraction and emission spectroscopy, and qualitatively by energy dispersive X-ray analysis. The microstructure of broken surfaces was examined in the scanning electron microscope.

0022–2461/87 $03.00 + .12

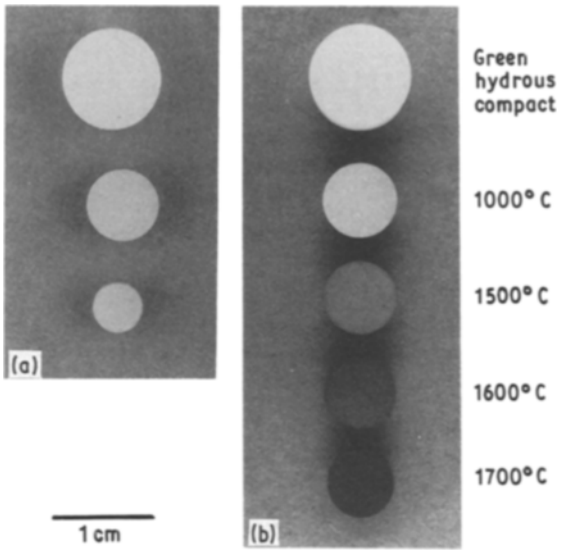

Figure 1 Green pellet of aluminium hydroxide and sintered pellets of alumina with (a) chromium and (b) molybdenum additions.

3. Results

The visual appearance of the original hydrous compacts and the sintered pellets of both chromium- and molybdenum-containing alumina is shown in Fig. 1. The pellets of both systems seem to shrink and densify without spalling or cracking, despite the loss in mass due to degradation of hydroxide to oxide phase. As a result of this transformation the weight loss in the neighbourhood of 800° C approximates 40% for the Cr–Al oxide system and 54% for the Mo–Al oxide system. This change in mass exceeds the calculated weight of the hydrous component in metal hydroxide and thus points to additional contributions by the metal contaminants in the vapour phase. The thermodynamic stabilities [20] seem to indicate molybdenum and chromium as the more probable metal contaminants in the vapour. However, with increases in temperature, in the interval 800 to 1700° C, the EDAX spectra revealed no loss of molybdenum component, whose concentration as determined by X-ray powder diffraction [21] at 1700° C (Fig. 2) is 0.12 mol %. In the case of the Cr_2O_3–Al_2O_3 mixture, chromia continued to vaporize in the reducing atmosphere with temperature (Fig. 3) and the emission spectroscopic results have shown changes in chromia content from 6 mol % at 1000° C to 3.5 mol % at 1700° C.

Some of the important features of the X-ray powder diffraction pattern are: the formation of alpha allotrope without the occurrence of the low-temperature gamma polymorph [16], broader alpha-phase reflections with chromium addition at 1000° C, solid solution of Cr_2O_3–Al_2O_3 over the entire temperature range, transformation of MoO_3–Al_2O_3 solid solution to Mo–Al_2O_3 composite with segregation of bcc molybdenum metal at temperatures above 1400° C, and loss in the X-ray intensity of chromia–alumina at a higher temperature of 1700° C. The average crystallite size determined by broadened X-ray lines [21] at 1000° C is nearly 10 nm for Cr_2O_3–Al_2O_3, and pure Al_2O_3 [16, 18], and 33 nm for MoO_3–Al_2O_3.

The temperature dependence of density, starting from a value of nearly 25% theoretical (th) at 800° C is shown in Fig. 4. From the comparison of these trends with respect to pure alumina (Fig. 4) that was also similarly synthesized with the exception of being calcined to the oxide phase [16], it appears that additions of molybdenum and chromium have an opposing effect of retarding and enhancing densification. For example, the densities at 1600° C are 98%, 44% and 30%th for Cr_2O_3–Al_2O_3, Al_2O_3, and Mo–Al_2O_3, respectively (Fig. 4).

Associated with density differences are the variations in the microstructure. Fig. 5 shows the difference in the agglomerate structure of the three oxides at 1000° C. Within the same porous compact of chromia–alumina the agglomerates seem to vary in size and Figs 5a and b show the two distinct size distributions. Both the agglomerate and inter-agglomerate voids are uniformly distributed, and the typical directional linkage among agglomerates to form rods or chains, observed in the other two oxides (Figs 5c and d) is absent in chromia–alumina. With increases in temperature the chromia–alumina microstructure evolves as shown in Fig. 6. The densification seems to be accompanied by elimination of intragranular features such as sub-grain boundaries and grooved linear features (Fig. 6a), by coarsening of intragranular

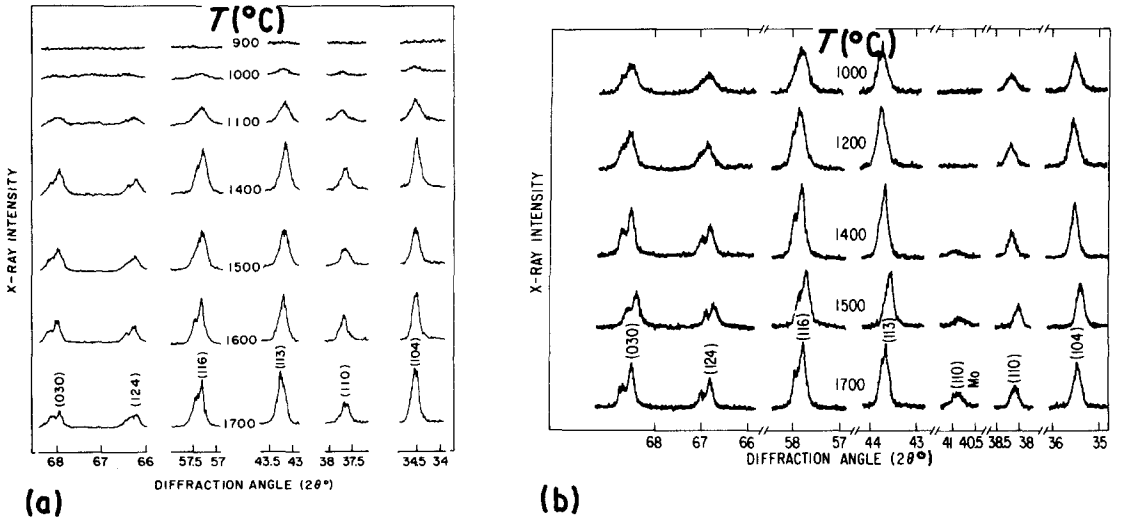

Figure 2 X-ray (Cu$K\alpha$) powder diffraction of sintered pellets of (a) chromium- and (b) molybdenum-containing aluminium oxide.

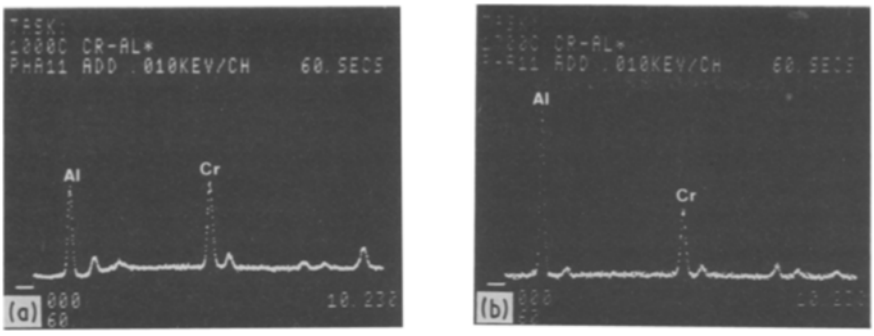

Figure 3 EDAX spectra of variations in Al/Cr ratio in the 1000 to 1700° C interval. (a) Chromia–alumina, T = 1000° C, 85 mol % Al_2O_3. (b) Chromia–alumina, T = 1700° C, 96.5 mol % Al_2O_3.

micropores (Figs 6b and c), by formation of elongated cavities near the grain boundary at 1600° C (Fig. 6b) and in the volume of the grain at 1700° C (Fig. 6c), and by pore-grain-boundary breakaway with the commencement of exaggerated growth at 1700° C (Fig. 6d).

In Mo–Al_2O_3 the exsolved molybdenum particles appear to decorate the grains and grain boundaries (Fig. 7a). Besides being randomly scattered within the grains they are linearly or helically arranged (regions marked x and y in Fig. 7). Molybdenum particles also occur in the core of triangular pits (z, Fig. 7). These pits are observed both on free and fractured grain surfaces. The pits are aligned and identical in size and shape. Some of the molybdenum particles seem to have overgrown and under high magnification are observed as protrusions (Fig. 7b). The EDAX shows molybdenum concentration in the protrusion (Fig. 7c) and its depletion in the neighbouring matrix (Fig. 7d). The high concentration of aluminium in Fig. 7c perhaps arises from the X-ray scan over a volume that is larger than the molybdenum phase. The elements of gold, copper and chromium in these spectra (Figs 7c and d) originate from the conductive coating and impurity in the furnace.

4. Discussion

The results suggest that the sintering process is activated [23] by two types of atmosphere. These are the metal-contaminated hydrous vapour and solute atmospheres [9, 11] of chromia-vacancy and molybdenum particles. The role of the former atmosphere is predominant in the course of transformation of hydrous phase to oxide, during which there is considerable shrinkage in the low-temperature regime

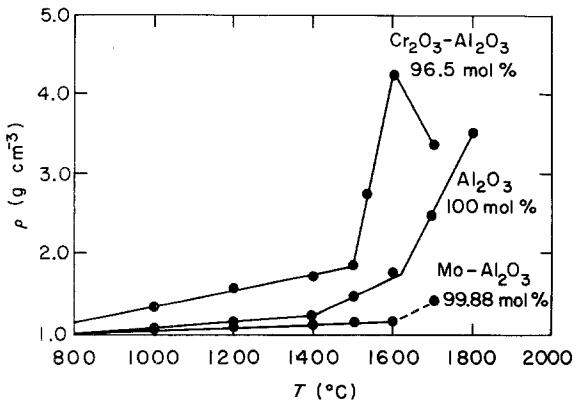

Figure 4 Temperature dependence of density.

from ambient to 1000° C (Fig. 1). Evidently, the hydrous vapour causes particle rearrangement within the porous compact, perhaps through capillary drag. The pellet of chromia–alumina is thus composed of uniform channels between the agglomerates (Figs 5a and b). In the course of the random path traced by the escaping fluid phase, there is the chance probability that the moving solid particles may coalesce and grow by condensation of the metallic components from the vapour. Considering the nearly spherical growth of the agglomerates (Fig. 6b) it may be suggested that condensation is one of adsorption. In the regions of porous compact where adsorption is predominant one would expect less capillary drag and therefore less shrinkage. In other regions where the vapour phase negligibly adheres to the particles, again capillary drag and shrinkage would be minimum. The transition in adsorption between these two extreme conditions is probably related to entropic interactions [24] among the solid and fluid particles and is the likely cause for shrinkage as well as particle growth. Thus, the agglomerates in Figs 5a and b of the same porous compact are examples of diminished and enhanced adsorption. Because of the interplay of capillary drag and adsorption, the evaporation–condensation mechanism invoked here contrasts from the conventional one that would introduce particle coarsening with negligible shrinkage [21, 25].

When molybdenum is added to alumina and the hydrous vapour is allowed to escape under the same heat treatment as for chromia–alumina, the pellet again, shows considerable shrinkage, although the agglomerate structure at 1000° C (Fig. 5c) is significantly different. Since, the common valency state of molybdenum is 6+ [19], and X-ray diffraction results show no phase segregation at lower temperatures (Fig. 2), it appears that in the solid solution MoO_3–Al_2O_3, point defects may originate with substitution of Mo^{6+} for Al^{3+}. It is probable that agglomerate hardening through grain growth, is initiated early in the sintering stage with molybdenum addition, by volume diffusion in the presence of point defects. Accordingly, the crystallites (Fig. 2) in MoO_3–Al_2O_3 are larger (33 nm) than in chromia–alumina ($\simeq$ 10 nm) at 1000° C.

Presence of alpha reflections at 1000° C (Fig. 2) is favoured by the octahedral site preference energy for both molybdenum and chromium [26]. Thus, alpha phase is stabilized below the gamma/alpha phase transformation temperature of 1200° C [27–29] because of elimination of the four-fold coordination [16] needed

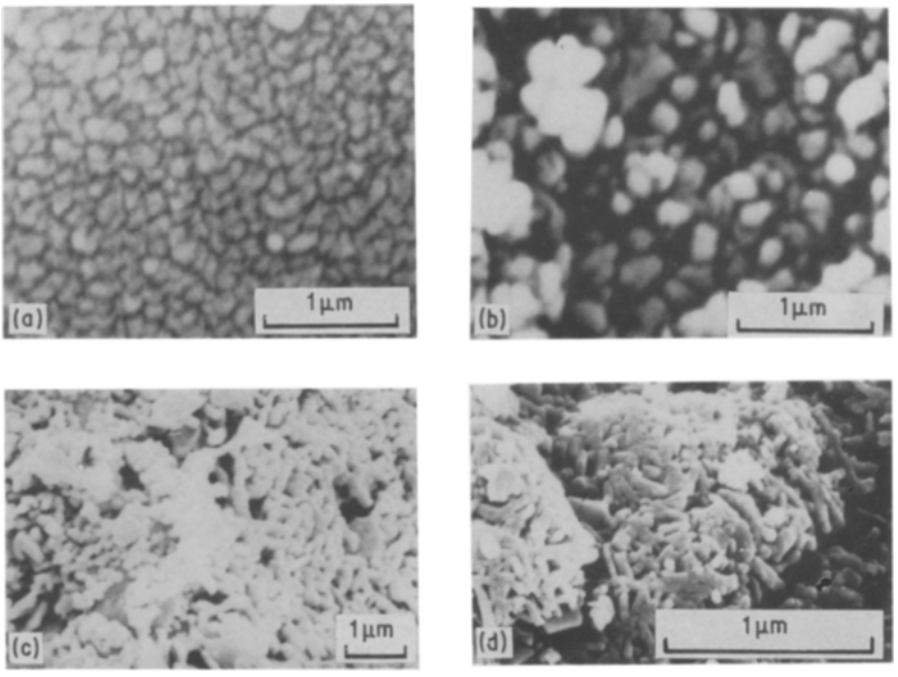

Figure 5 Scanning electron micrographs of the porous compact at 1000° C. (a), (b) Cr_2O_3–Al_2O_3, (c) MoO_3–Al_2O_3, and (d) Al_2O_3.

for forming gamma phase. Although, with the removal of gamma phase one would expect avoidance of shrinkage retardation, induced by phase transformation [16] the densification in the initial stage is dominated by agglomerate structure. The similar clustered rodlet structures in MoO_3–Al_2O_3 (Fig. 5c) and pure gamma alumina (Fig. 5d) lead to the same type of densification (Fig. 4), despite the crystallochemical differences such as the presence of point defects in MoO_3–Al_2O_3 and gamma/alpha phase transformation in alumina. It may be suggested that the structure composed of soft agglomerates [30] and uniformly distributed inter-agglomerate pores like the ones observed in chromia–alumina (Figs 5a and b) contributes more to densification (Fig. 4). This implies that the heating-rate controlled evaporation–condensation could be an important preceding mechanism for improved densification in the absence of point defects.

At higher temperatures the densification seems to be influenced by the presence of defect structures. The defects of interest are vacancy clusters, sub-grain boundaries and dislocations. These features can generally be revealed by segregated nucleation and growth of solute atmospheres such as vacancies and chemical impurities, through etching or preferred heat treatments in crystallographically incoherent areas [9–13]. In chromia–alumina solid solution, it is possible that the vacancy atmosphere is imparted to the lattice through partial vaporization of chromia (Fig. 3) during sintering under reducing conditions. The scanning electron micrograph thus reveals chromia-vacancy segregations along sub-grain boundaries,

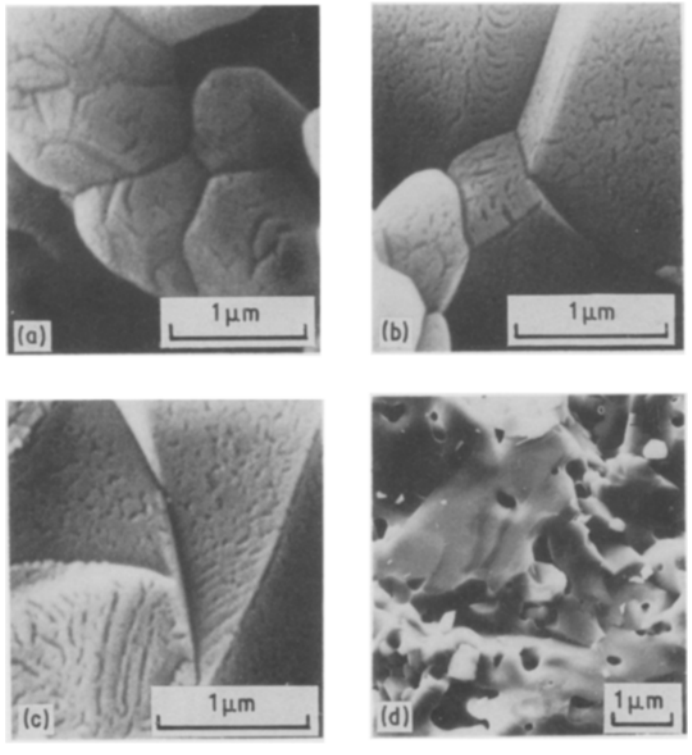

Figure 6 Scanning electron micrographs of Cr_2O_3–Al_2O_3. (a) 1500° C, (b) 1600° C, (c) and (d) 1700° C.

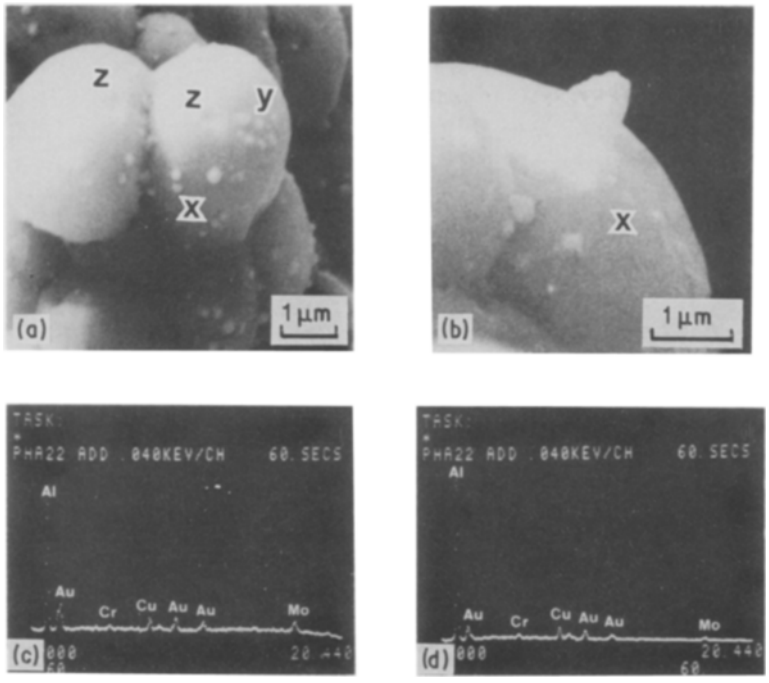

Figure 7 (a), (b) Scanning electron micrographs of $Mo-Al_2O_3$, molybdenum particles are arranged linearly near x and helically near y, and occur in the core of triangular pits z. (c) EDAX of molybdenum protrusion in (b), and (d) EDAX of matrix near the protrusion.

along linear and sickle-shaped intragranular features that are reminiscent of dislocations [14, 15], and along randomly scattered intragranular cavities. Considering the increased loss of chromia (Fig. 3) the growth of cavities [8, 31] with temperature (Fig. 6) may be attributed to condensation of excess chromia-vacancies. The transformation of these isolated features to elongated type initially, near the grain boundary at 1600° C (Fig. 6b) and then their extension into the volume of the grain at 1700° C (Fig. 6c) with change in the grain-boundary shape perhaps, points to the presence of creep-induced stresses for flux of defects [32, 33] during transition from grain-boundary to volume-diffusion creep mechanisms (Coble to Nabarro–Herring creep) [20]. It seems that the exaggerated growth in the form of pore-grain-boundary breakaway (Fig. 6d) and trifle variations in X-ray reflections (marginal shifts in *d*-spacings and loss in intensity, Fig. 2) in proceeding from 1600 to 1700° C are associated with such mechanistic changes. In view of the possibility of reduction in valency of chromium from 3+ to 2+ with temperature increase under reducing conditions, it may be suggested that Jahn–Teller distortions in coordination octahedra [26] are sensed by the X-ray diffraction and contribute to Nabarro–Herring plasticity [20, 34] in alumina above 1600° C. This supports the enhanced mobility of the grain boundary and exaggerated growth. The desintered density (85%th) at 1700° C (Fig. 4) with accompanying reduction in shrinkage and formation of oblong pores suggests that pore mobility in the grains is an interplay of lattice diffusivity and gaseous pore pressure [8], which is activated by chromia vaporization and external stress arising from the Jahn–Teller effect.

The defects of dislocation core and vacancy clusters would offer a more matching vacant space for the neutral molybdenum solute, that is rejected by alumina with increase in temperature under reducing conditions (Fig. 7). In view of the relatively distant spacing of dislocation edges in the sub-grain boundary than in the high-angle grain boundary [35] it may be suggested that extended linear spacing of molybdenum particles on the free grain surface (Figs 7a and b) and their crowding along the grain boundary (Fig. 7a) points to a dislocation origin for these planar features. The growth of molybdenum particles on the free surface through dislocation pipe diffusion [35, 36] can be supported by the existence of molybdenum protrusions (Fig. 7b) and triangular pits (Fig. 7a), whose cores are occupied by molybdenum particles both on free and broken grain surfaces. From the comparison of microstructures, one would note that the density differences (Fig. 4) relative to pure alumina, seem to be related (among other causes) to annihilation of sub-grain boundaries and dislocations in chromia–alumina (Fig. 6) and locking of the mobility of these features by bcc molybdenum (Fig. 7) in molybdenum–alumina composite.

Acknowledgements

It is my pleasure to thank Professor R. H. Doremus, Dr M. Suenaga and Mr R. Sabatini for encouraging this work in their laboratories.

References

1. C. O. McHUGH, T. J. WHALEN and M. HUMENIK Jr, *J. Am. Ceram. Soc.* **49** (1966) 486.
2. R. C. BRADT, *ibid.* **50** (1967) 54.
3. J. R. HENSLER and E. C. HENRY, *ibid.* **36** (1953) 76.
4. R. L. COBLE, *J. Appl. Phys.* **32** (1961) 787.
5. *Idem, ibid.* **32** (1961) 793.
6. D. L. JOHNSON and I. B. CUTLER, *J. Am. Ceram. Soc.* **46** (1963) 545.
7. P. L. JORGENSEN, *ibid.* **48** (1965) 207.
8. S. J. BENNISON and M. P. HARMER, *ibid.* **68** (1985) 591.
9. A. H. COTTRELL, in "Relation of Properties to Microstructure", 35th Metal Congress (Americal Society for Metals, Cleveland, Ohio, 1953) p. 131.
10. J. J. GILMAN and W. G. JOHNSTON, *J. Appl. Phys.* **27** (1956) 1018.
11. J. W. CAHN, *Acta Metall.* **10** (1962) 789.

12. H. J. LEVINSTEIN and H. J. GUGGENHEIM, *Trans. TMS-AIME* **245** (1969) 375.
13. C. W. LI and W. D. KINGERY, in "Structure and Properties of MgO and Al_2O_3 Ceramics", edited by W. D. Kingery, Advances in Ceramics, Vol. 10 (American Ceramic Society, Columbus, Ohio, 1984) p. 368.
14. K. J. MORRISSEY and C. B. CARTER, in "Character of Grain Boundaries", edited by M. F. Yan and A. H. Heuer, Advances in Ceramics, Vol. 6 (American Ceramic Society, Columbus, Ohio, 1983) p. 85.
15. A. H. HEUER and J. CASTAING, in "Structure and Properties of MgO and Al_2O_3 Ceramics", edited by W. D. Kingery, Advances in Ceramics, Vol. 10 (American Ceramic Society, Columbus, Ohio, 1984) p. 238.
16. S. V. RAMAN, R. H. DOREMUS and R. M. GERMAN, in "Sintering and Heterogeneous Catalysis", edited by G. C. Kuczynski, A. E. Miller and G. A. Sargent Materials Science Research, Vol. 16 (Plenum, New York, 1984) p. 253.
17. T. E. MITCHELL, K. P. D. LAGERLOF and A. H. HEUER, *Mater. Sci. Tech.* **1** (1985) 944.
18. S. V. RAMAN, R. H. DOREMUS and R. M. GERMAN, *J. Physique C1* **47** (1986) 225.
19. F. D. BLOSS, "Crystallography and Crystal Chemistry", 1st edn (Holt, Rinehart and Winston, New York, 1971) p. 183.
20. W. D. KINGERY, H. K. BOWEN and D. R. UHLMANN, "Introduction to Ceramics", 2nd edn (Wiley, New York, 1976) p. 381.
21. D. W. READY, J. LEE and T. QUADIR, in "Sintering and Heterogeneous Catalysis", edited by G. C. Kuczynski, A. E. Miller and G. A. Sargent, Materials Science Research, Vol. 16 (Plenum, New York, 1984) p. 115.
22. B. D. CULLITY, "Elements of X-ray Diffraction" (Addison-Wesley, Reading, Massachusetts, 1967) p. 99.
23. A. J. SHALER, in "Sintering and Related Phenomena", edited by G. C. Kuczynski, N. A. Hooton and C. F. Gibbon (Gordon and Breach, New York, 1967) p. 807.
24. D. E. SULLIVAN, *Phys. Rev. B* **20** (1979) 3991.
25. W. D. KINGERY and M. BERG, *J. Appl. Phys.* **26** (1955) 1205.
26. R. G. BURNS, "Mineralogical Applications of Crystal Field Theory", 1st edn (Cambridge University Press, London, 1970) p. 224.
27. C. J. P. STEINER, D. P. H. HASSELMAN and R. M. SPRIGGS, *J. Amer. Ceram. Soc.* **54** (1971) 412.
28. G. C. BYE and G. T. SIMPKIN, *ibid.* **57** (1974) 367.
29. F. W. DYNYS and J. W. HALLORAN, in "Ultrastructure Processing of Ceramics, Glasses and Composites", edited by L. L. Hench and D. R. Ulrich (Wiley, New York, 1984) p. 142.
30. J. W. HALLORAN, *ibid.* p. 404.
31. N. J. TIGHE, S. M. WIEDERHORN, T. J. CHUANG and C. L. McDANIEL, in "Deformation of Ceramic Materials II", edited by R. E. Tressler and R. C. Bradt, Materials Science Research, Vol. 18 (Plenum, New York, 1984) p. 587.
32. A. L. RUOFF, *J. Appl. Phys.* **21** (1950) 2903.
33. D. W. READY, *J. Amer. Ceram. Soc.* **49** (1966) 366.
34. C. HERRING, *J. Appl. Phys.* **21** (1950) 301.
35. N. L. PETERSON, in "Characterization of Grain Boundaries", edited by M. F. Yan and A. H. Heuer, Advances in Ceramics, Vol. 6 (American Ceramic Society, Columbus, Ohio, 1983) p. 236.
36. J. NARAYANAN and J. WASHBURN, *Acta Metall.* **21** (1973) 533.

Received 26 August
and accepted 9 October 1986